# Effect of an $S_1/S_0$ Conical Intersection on the Chemistry of Nitramide in Its Ground State. A Comparative CASPT2 Study of the Nitro-Nitrite Isomerization Reactions in Nitramide and Nitromethane

**Juan Soto,* Juan F. Arenas, Juan C. Otero, and Daniel Peláez**

*Department of Physical Chemistry, Faculty of Sciences, University of Málaga, E-29071 Málaga, Spain*

*Received: March 20, 2006; In Final Form: May 10, 2006*

The potential energy surfaces for the dissociation of nitramide ($NH_2NO_2 \rightarrow NH_2 + NO_2$) and nitromethane ($CH_3NO_2 \rightarrow CH_3 + NO_2$) and the nitro-nitrite rearrangement of these nitrocompounds ($RNO_2 \rightarrow RONO$) as well as the dissociations of the nitrite isomers ($RONO \rightarrow RO + NO$) have been studied with the second-order multiconfigurational perturbation theory (CASPT2) by computation of numerical energy gradients for stationary points. It is found that multiconfigurational methods [CASPT2 and complete active space SCF (CAS−SCF)] predict that the isomerization of nitramide to $NH_2ONO$ occurs in a two-step mechanism: (i) $NH_2NO_2 \rightarrow NH_2 + NO_2$ and (ii) $NH_2 + NO_2 \rightarrow NH_2ONO$, the second step involving surmounting an activation barrier. Contrastingly, Hartree−Fock based approaches give isomerization as a one-step reaction. Additionally, both mono- and multiconfigurational methods predict that nitro-nitrite rearrangement of $CH_3NO_2$ is a one-step process. The difference in the reaction mechanisms of these two isoelectronic molecules arises from the presence of an $S_1/S_0$ conical intersection in nitramide which is absent in nitromethane.

## Introduction

It is firmly established that conical intersections are key features in the photochemistry of polyatomic molecules.[1,2] One of their most important implications is that internal conversion from upper to lower excited states occurs efficiently through or near these crossing points. On the other hand, it is commonly asserted that upward transitions from the lower surface to the upper surface should be less likely because there exists a peak in the lower surface which tends to guide trajectories away from the intersection.[3−5] Therefore, the role of surface crossings for the chemistry of molecules in the ground state should be less important. Otherwise, there are several cases in which conical intersections are relevant in the chemistry of molecules even in the ground state. These cases correspond to the so-called diabatic trapping effect, which implies nonadiabatic recrossing of the potential energy surfaces.[5−11]

The present work reports how the existence of an $S_1/S_0$ conical intersection determines the chemistry of nitramide ($NH_2NO_2$) in its ground state. The observed effect consists of the distortion of the ground-state potential energy surface by the conical intersection. Such a topological alteration of the surface extends to a wide region and leads to a dramatic change in the expected reaction mechanism. It must be noticed that a diabatic trap is not invoked at all.

To enlighten this effect, we must compare the reaction mechanisms for nitro-nitrite isomerizations of nitromethane ($CH_3NO_2 \rightarrow CH_3ONO$) and nitramide ($NH_2NO_2 \rightarrow NH_2ONO$). Great attention has been paid to these reactions in computational studies[12−20] since the pioneer work of Dewar et al.[12] on the rearrangement of nitromethane to methylnitrite ($CH_3ONO$). The infrared multiphoton dissociation experiments of Wodtke, Hintsa, and Lee[21] indicate that isomerization of nitromethane (eq 1) is a one-step reaction competing with C−N bond dissociation (eq 2). A transition state exists in the isomerization reaction, while dissociation does not exhibit any exit energy barrier.

$$CH_3NO_2 \rightarrow CH_3ONO \quad (1)$$

$$CH_3NO_2 \rightarrow CH_3 + NO_2 \quad (2)$$

The accepted reaction mechanisms for nitramides give the same pictures. That is

$$NH_2NO_2 \rightarrow NH_2ONO \quad (3)$$

$$NH_2NO_2 \rightarrow NH_2 + NO_2 \quad (4)$$

In this study we demonstrate that the nitro-nitrite rearrangement of nitramide occurs in a two-step mechanism (5) that implies dissociation into $NH_2 + NO_2$ and subsequent recombination of the radicals after surmounting an energy barrier. In contrast, nitro-nitrite isomerization of nitromethane takes place in only a one-step reaction. The reason for this different mechanistic behavior of nitramide with respect to that of nitromethane arises from the presence of an $S_1/S_0$ conical intersection in nitramide which is absent in nitromethane.

$$NH_2NO_2 \rightarrow NH_2 + NO_2 \rightarrow NH_2ONO \quad (5)$$

## Computational Details

Generally contracted basis sets of atomic natural orbital (ANO) type obtained from C,N,O(14*s*9*p*4*d*3*f*)/H(8*s*4*p*3*d*) primitive sets,[22] the so-called ANO-L basis sets, with the C,N,O-[4*s*3*p*2*d*1*f*]/H[3*s*2*p*1*d*] contraction schemes, were used in all of the geometry optimizations of the relevant species involved in the reactions of nitromethane and nitramide. These optimizations were performed following two strategies: (i) optimization at the complete active space self-consistent field (CAS−SCF)[23]

* Corresponding author e-mail: soto@uma.es.

10.1021/jp0617219 CCC: $33.50 
Published on Web 06/10/2006

level of theory by computation of analytical energy gradients and (ii) optimizations with the second-order multiconfigurational perturbation theory (CASPT2)[24] by computation of numerical energy gradients. Both methods were applied as implemented in the MOLCAS 6.2 program.[25] In the CASPT2 calculation, the 1*s* electrons of the carbon, oxygen, and nitrogen atoms, as determined in the SCF calculations, were kept frozen. On the other hand, the localization of the crossing points was done with the algorithm implemented in the GAUSSIAN program[26] and with the cc-pVDZ basis sets.[27] The gradient difference and nonadiabatic coupling vectors are computed by using state average orbitals in the manner suggested by Yarkony.[28]

The stationary points (minima and saddle points) were characterized by their CASSCF analytic harmonic vibrational frequencies computed by diagonalizing the mass-weighted Cartesian force constant matrix.

The selection of the active space plays a critical role in the CAS−SCF studies of nitromethane and nitramide. If we want to avoid undesirable effects such as symmetry breaking when the systems move on the potential energy surfaces, the minimum active space must comprise 14 electrons distributed in 11 orbitals.[29] These orbitals correspond to $2s_N$, two NO bonding orbitals $\sigma$NO, one delocalized ONO $\pi$-bonding orbital $\pi$NO, one $\sigma$ nonbonding orbital n$\sigma$O, one $\pi$ nonbonding orbital n$\pi$O, two NO antibonding orbitals $\sigma^*_{NO}$, one delocalized ONO $\pi$-antibonding orbital $\pi^*_{NO}$, plus CN bonding and antibonding orbitals $\sigma$CN and $\sigma^*_{CN}$ on $CH_3NO_2$ or NN bonding and antibonding orbitals $\sigma$NN and $\sigma^*_{NN}$ orbitals on $NH_2NO_2$, respectively.

## Results and Discussion

This section is organized as follows. Prior to discussion of the reaction mechanisms, all of the critical points found in this study are illustrated in Figure 1, which have been plotted with the MacMolplt program.[30] Second, it is shown that the dissociation reactions of the four isoelectronic molecules dealt with in this work ($CH_3NO_2$, $CH_3ONO$, $NH_2NO_2$, and $NH_2ONO$) occur without any exit energy barrier. Third, the nitro-nitrite isomerization reactions of nitromethane ($CH_3NO_2 \rightarrow CH_3ONO$) and nitramide ($NH_2NO_2 \rightarrow NH_2ONO$) are discussed, respectively. Comparison of both reaction mechanisms will allow us to obtain the main conclusion of this work.

**Conformers on the Potential Energy Surfaces of the Nitro and Nitrite Compounds.** Nitromethane has two $C_s$ conformers: (i) staggered (M1, Figure 1a) and (ii) eclipsed. They are almost isoenergetic but with the staggered structure slightly favored. Methylnitrite has four conformational isomers with $C_s$ symmetry depending on whether the terminal NO and in-plane hydrogen are placed cis or trans with respect to the central NO bond: (i) trans−trans (M2, Figure 1b), (ii) trans−cis, (iii) cis−trans, and (iv) cis−cis. The cis−trans conformer is energetically the most stable one (Table 1). The cis−cis isomer is a saddle point on the potential energy surface at the CAS−SCF level.

Nitramide has only one $C_s$ conformer (M3, Figure 1d). As methylnitrite, there are four isomers of $NH_2ONO$ depending on whether the terminal NO and hydrogens are placed cis or trans with respect to the central NO bond. The cis−cis isomer is the most stable one (Table 2). In Figure 1e we show the trans−trans conformer.

**$NO_2$ and NO Eliminations.** We have studied dissociations of the nitro and nitrite compounds by calculating the energy profiles of the reactions along linear interpolations as in previous works.[29,31] That is, an interpolation vector, $\Delta\boldsymbol{R}$, which connects ground states of stable molecules and their respective dissociation products, is obtained by calculating the difference between internal coordinates of reactant and dissociation products, $\Delta\boldsymbol{R} = \boldsymbol{R}_i - \boldsymbol{R}_j$, where $\boldsymbol{R}_i$ and $\boldsymbol{R}_j$ represent the internal coordinate vectors of the initial and dissociation products, respectively. Units of the interpolation vector are measured in Å for internuclear distances and degrees for valence and dihedral angles.

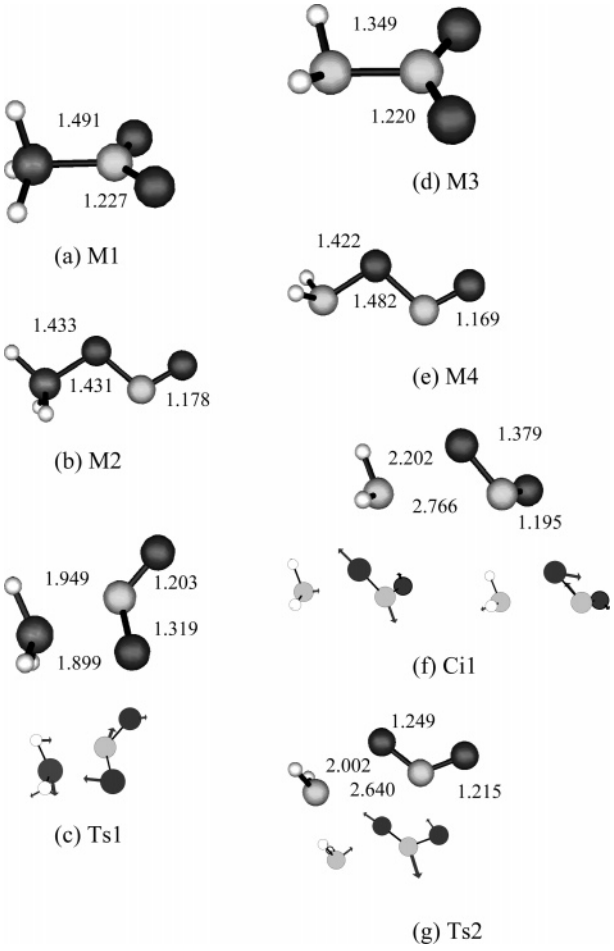


**Figure 1.** CASPT2 geometries of the relevant species for the decomposition and isomerization of both nitromethane and nitramide: (a) staggered nitromethane (M1); (b) trans−trans methyl nitrate (M2); (c) transition state for M1 → M2 isomerization (Ts1), the arrows in the smaller figures correspond to the transition vector; (d) nitramide (M3); (e) trans−trans $NH_2ONO$ (M4); (f) S1/S0 conical interaction (Ci1), the arrows in the smaller figures correspond to nonadiabatic coupling (left) and gradient difference (right) vectors; (g) transition state for M3 → M4 isomerization (Ts2), the arrows in the smaller figures correspond to the transition vector.

Figure 2 displays the energy profiles for dissociation of $CH_3NO_2$ and $CH_3ONO$ into $CH_3 + NO_2$ and $CH_3O + NO$, respectively. The $S_1$ state for dissociation of $CH_3ONO$ is also plotted in the same figure, which shows that $S_1$ is dissociative.

Figure 3 shows the energy profiles for dissociation of $NH_2NO_2$ and $NH_2ONO$ into $NH_2 + NO_2$ and $NH_2O + NO$, respectively. As occurs in $CH_3ONO$, the $S_1$ state of $NH_2ONO$ results in being dissociative.

The two-dimensional plots given in Figures 2 and 3 are not true reaction paths but cuts of the multidimensional potential energy surfaces along an arbitrary direction. However, provided that no barrier is found along these dissociation interpolations, it should not exist along the true energy paths. In other words, there will not be saddle points related to transition states on the potential energy surfaces.

**TABLE 1: Energetic of the Critical Points on the $S_0$ Potential Energy Surfaces of $CH_3NO_2$[a]**

| description | CASPT2[a] | ZPE[b,c] | TC[c,d] | $\Delta H$[e] | exp.[h] |
|---|---|---|---|---|---|
| *s*-$CH_3NO_2$ | −244.620 77 | 29.2 | 2.3 | 0.0 | |
| | | (30.2)[g] | (2.2) | (0.0) | |
| *e*-$CH_3NO_2$ | −244.620 79 | 29.2 | 2.8 | 0.6 | |
| *t*-*t*-$CH_3ONO$, m[j] | −244.612 24 | 28.1 | 3.2 | 5.2 | |
| *t*-*c*-$CH_3ONO$, m[j] | −244.612 65 | 28.1 | 2.6 | 4.3 | |
| *c*-*t*-$CH_3ONO$, m[j] | −244.614 49 | 28.5 | 2.9 | 3.9 | 1.36 |
| *c*-*c*-$CH_3ONO$, sd[k] | −244.611 54 | 28.2 | 2.5 | 5.1 | |
| Ts1 | −244.509 64 | 26.6 | 3.0 | 67.8 | |
| $CH_3 + NO_2$[f] | −244.519 66 | 22.0 | 4.0 | 58.6 | 60.89[i] |
| | | (23.5) | (3.7) | (58.8) | |
| $CH_3O + NO$[f] | −244.542 08 | 23.0 | 3.7 | 43.9 | 41.87[i] |

[a] CASPT2/ANO-L energy in hartrees. [b] Zero point energy in kcal/mol. [c] Vibrational frequencies scaled by 0.90. [d] Thermal correction (298.15 K) in kcal/mol. [e] Relative enthalpies in kcal/mol with respect to the ground state of *s*-$CH_3NO_2$. [f] Distance between fragments 10 Å. [g] In parentheses values obtained including experimental frequencies. [h] From: In *CRC Handbook of Chemistry and Physics*, 67th ed. 1986−1987; Weast, R. C., Ed.; CRC Press: Boca Raton, FL, 1986. [i] Bond dissociation energy calculated as $D° = \sum\Delta_f H°(\text{product}) - \Delta_f H°(\text{reactant})$. [j] m: minimum. [k] sd: saddle point.

**TABLE 2: Energetic of the Critical Points on the $S_0$ Potential Energy Surfaces of $NH_2NO_2$[a]**

| description | CASPT2[a] | ZPE[b,c] | TC[c,d] | $\Delta H$[e] |
|---|---|---|---|---|
| $NH_2NO_2$ | −260.642 70 | 23.2 | 2.5 | 0.0 |
| *t*-*t*-$NH_2ONO$, m[i] | −260.604 58 | 21.6 | 3.0 | 22.9 |
| *t*-*c*-$NH_2ONO$, m[i] | −260.603 56 | 21.6 | 3.0 | 23.5 |
| *c*-*t*-$NH_2ONO$, m[i] | −260.605 58 | 21.5 | 3.0 | 22.2 |
| *c*−*c*-$NH_2ONO$, m[i] | −260.607 83 | 21.8 | 2.8 | 20.9 |
| Ts2 | −260.541 42 | 17.6 | 3.5 | 58.9 |
| Ci1 $S_1/S_0$ | −260.515 10[f] | - | - | 80.5 |
| $NH_2 + NO_2$[g] | −260.557 13 | 15.3 | 3.6 | 47.6 |
| $NH_2O + NO$[g] | −260.581 48[h] | 17.5 | 3.6 | 36.2 |

[a] CASPT2/ANO-L energy in hartrees. [b] Zero point energy in kcal/mol. [c] Vibrational frequencies scaled by 0.90. [d] Thermal correction (298.15 K) in kcal/mol. [e] Relative enthalpies in kcal/mol with respect to the ground state of *s*-$NH_2NO_2$ [f] Multistate-CASPT2 energy referred to −260.643 42 hartrees [reference wave function CAS(14,12), 2 roots]. [g] Distance between fragments 10 Å. [h] Multistate-CASPT2 energy referred to −260.645 40 hartrees [reference wave function CAS(16,12), 4 roots]. [i] m: minimum.

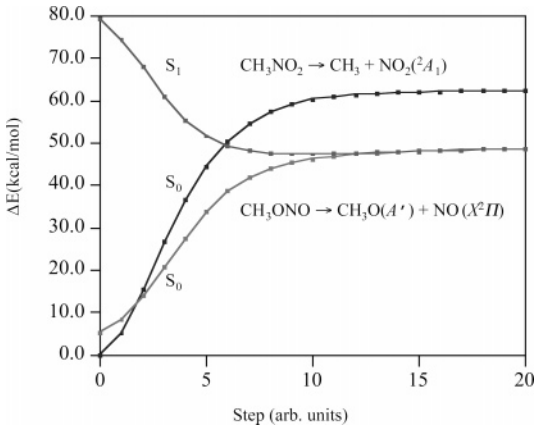


**Figure 2.** Singlet CASPT2/ANO-L dissociation curves ($C_s$ symmetry) of nitromethane ($S_0$) and trans−trans methyl nitrate ($S_0$ and $S_1$). The geometry of the initial points corresponds to the minima of nitromethane and methyl nitrite, respectively.

**$NO_2$-ONO Rearrangement of $CH_3NO_2$ and $NH_2NO_2$.** Isomerization of nitromethane (M1, Figure 1a) to methylnitrite (M2, Figure 1b) occurs in a one-step reaction after passing through a transition state (Ts1, Figure 1c) lying 68 kcal/mol above the $S_0$ minimum of nitromethane. The intrinsic reaction coordinate (IRC) starting at Ts1 leads to nitromethane and methylnitrite, respectively (Figure S1). The geometry and energetic of this CASPT2 transition state is in agreement with the structures reported by Nguyen et al.[16] using the CCSD(T) and CAS−SCF methods.

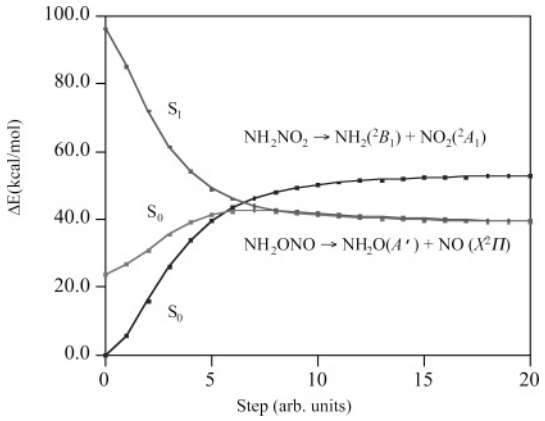


**Figure 3.** Singlet CASPT2/ANO-L dissociation curves ($C_s$ symmetry) of nitramide ($S_0$) and trans−trans $NH_2ONO$ ($S_0$ and $S_1$). The geometry of the initial points corresponds to the minima of nitramide and trans−trans $NH_2ONO$, respectively.

Nitro-nitrite rearrangement in nitramide deserves much attention. We were able to find the transition state for isomerization of nitramide (M3, Figure 1d) to $NH_2ONO$ (M4, Figure 1e) by applying different approaches: (i) restricted Hartree−Fock (RHF), (ii) restricted density functional theory (DFT), and (iii) restricted Møller−Plesset (MP2). The geometrical parameters of these transition states are collected in Table S1. As an example, Figure S2 shows the energy profile of the IRC starting at the saddle point found with the DFT/B3-LYP method. This IRC clearly demonstrates that this structure is the transition state for the nitro-nitrite rearrangement of nitramide at this level of theory.

Surprisingly, despite an exhaustive search, it was impossible at all to find the nitro-nitrite transition state of nitramide at the CAS−SCF and CASPT2 levels of theory. We expected to find such a transition state close to the geometry predicted by DFT methods. However, what we found in the neighboring of this region was an $S_1/S_0$ conical intersection (Ci1, Figure 1f). Minimum energy paths starting at this conical intersection and following both directions of the gradient difference and nonadiabatic coupling vectors always led the system to $NH_2ONO$ or dissociation products ($NH_2 + NO_2$), alternately.

To clarify the discrepancy found between multiconfigurational and Hartree−Fock based methods, the reduced three-dimensional potential energy surfaces for the isomerization reaction of nitramide have been built at the state averaged CAS−SCF level of theory including both the $S_0$ and $S_1$ states (Figure 4a) and applying the N,O[3*s*2*p*1*d*]/H[2*s*1*p*] contraction schemes to the ANO-L basis sets. The points which generate these surfaces span the geometries of four critical molecular arrangements: (i) nitramide (M3), (ii) $S_1/S_0$ conical intersection (Ci1), (iii) $NH_2$-ONO (M4), and (iv) dissociation products ($NH_2 + NO_2$). The most striking feature of this figure is the $S_1/S_0$ conical intersection. Additionally, a reaction path leading to the dissociation of nitramide into $NH_2 + NO_2$ on the $S_0$ surface is observed, but no transition state appears for the direct isomerization. The reason for this behavior can be attributed to the presence of such a conical intersection, which repels down the $S_0$ surface destroying the transition state for isomerization. On the other hand, the $S_0$ surface exhibits a saddle point near the conical intersection, which is located approximately along the

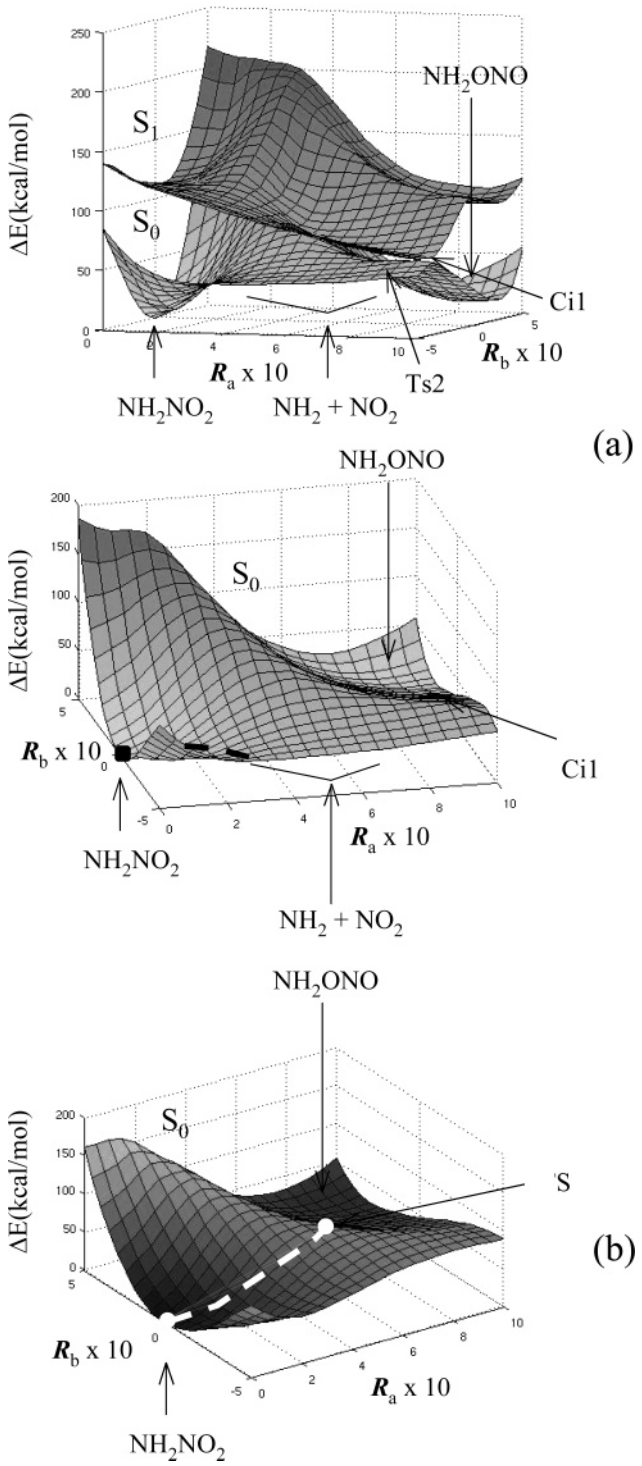


**Figure 4.** Potential energy surfaces for the $NH_2NO_2 \rightarrow NH_2ONO$ reaction (a) (upper) state average CAS-SCF/ANO-L (C,N,O[3*s*2*p*1*d*]/H[2*s*1*p*]) surfaces of the $S_1$ and $S_0$ states showing the $S_1/S_0$ conical intersection and (lower) $S_0$ surface from a different perspective and (b) $S_0$ B3-LYP/aug-cc-pvdz surface showing a saddle point between $NH_2NO_2$ and $NH_2ONO$.

line defined by $NH_2ONO$ and dissociation products. Thus, we searched for and localized a transition state in the vicinity of this region (Ts2, Figure 1g). The IRC starting at this stationary point demonstrates that it is the transition state for the bimolecular reaction $NH_2 + NO_2 \rightarrow NH_2ONO$ (Figure S3).

It is worthy to note that surfaces displayed in Figure 4 are built from a set of perfectly ordered points. The two orthogonal directions are obtained as follows:

(1) Two generator vectors are defined in internal coordinates as

$$\boldsymbol{R}_1 = \boldsymbol{R}(NH_2NO_2) - \boldsymbol{R}(NH_2ONO) \tag{6a}$$

$$\boldsymbol{R}_2 = \boldsymbol{R}(NH_2NO_2) - \boldsymbol{R}(Ci1) \tag{6b}$$

where $\boldsymbol{R}(I)$ denotes the internal coordinate vector of a given species.

(2) Vectors $\boldsymbol{R}_1$ and $\boldsymbol{R}_2$ are normalized

$$\boldsymbol{r}_1 = \frac{\boldsymbol{R}_1}{R_1} \tag{7}$$

$$\boldsymbol{r}_2 = \frac{\boldsymbol{R}_2}{R_2} \tag{8}$$

(3) Sum and subtraction of $\boldsymbol{r}_1$ and $\boldsymbol{r}_2$ give a set of two orthonormal vectors

$$\boldsymbol{r}_a = \boldsymbol{r}_1 + \boldsymbol{r}_2 \tag{9}$$

$$\boldsymbol{r}_b = \boldsymbol{r}_1 - \boldsymbol{r}_2 \tag{10}$$

(4) Vectors $\boldsymbol{r}_a$ and $\boldsymbol{r}_b$ are scaled by the length of the largest vector between $\boldsymbol{R}_1$ and $\boldsymbol{R}_2$, which is $\boldsymbol{R}_2$ in this case

$$\boldsymbol{R}_a = R_2 \cdot \boldsymbol{r}_a \tag{11}$$

$$\boldsymbol{R}_b = R_2 \cdot \boldsymbol{r}_b \tag{12}$$

The B3-LYP/aug-cc-pVDZ potential energy surface of the nitro-nitrite isomerization of nitramide (Figure 4b) has been built with the same geometrical points used in Figure 4a. Although the geometry of the transition state has not been specifically included, it is observed for the reaction path for direct isomerization passing through a saddle point in such a figure. This fact strengthens our confidence in that the reduced potential energy surfaces are representative of the reaction mechanisms. That is, if the transition state for isomerization does exist at the CAS−SCF level, we had been indeed able to find it. There are several reasons to think that the picture given for the isomerization process by the methods based on monoconfigurational wave functions are nothing but artifacts. First, the weight of the Hartree−Fock configuration on the multiconfigurational wave function amounts to ∼50% around the region of the conical intersection, just where restricted approaches localize the transition state. Second, these methods give an incorrect dissociation limit which topologically results on an overestimation of the energy of the lower right corner of Figure 4b. This fact, in connection with the two minima corresponding to $NH_2NO_2$ and $NH_2ONO$, creates an artificial saddle point. Third, monoconfigurational methods are blind to the $S_1$ state.

The same procedure has been applied to build the potential energy surfaces of the nitro-nitrite rearrangement of nitromethane (Figure 5). In this case, generator vectors ($\boldsymbol{R}_1$ and $\boldsymbol{R}_2$) are obtained as $\boldsymbol{R}_1 = \boldsymbol{R}(CH_3ONO) - \boldsymbol{R}(CH_3NO_2)$ and $\boldsymbol{R}_2 = \boldsymbol{R}(Ts1) - \boldsymbol{R}(CH_3NO_2)$, respectively. Figure 5 shows the $S_1$ and $S_0$ potential energy surfaces built at the state average CAS−SCF level applying the C,N,O[3*s*2*p*1*d*]/H[2*s*1*p*] contraction schemes to the ANO-L basis sets. It is observed that the saddle point related to the transition state for direct isomerization is actually well defined. Likewise, it is important to notice that $S_0$ and $S_1$ states do not touch each other in the whole region spanned by the surfaces.

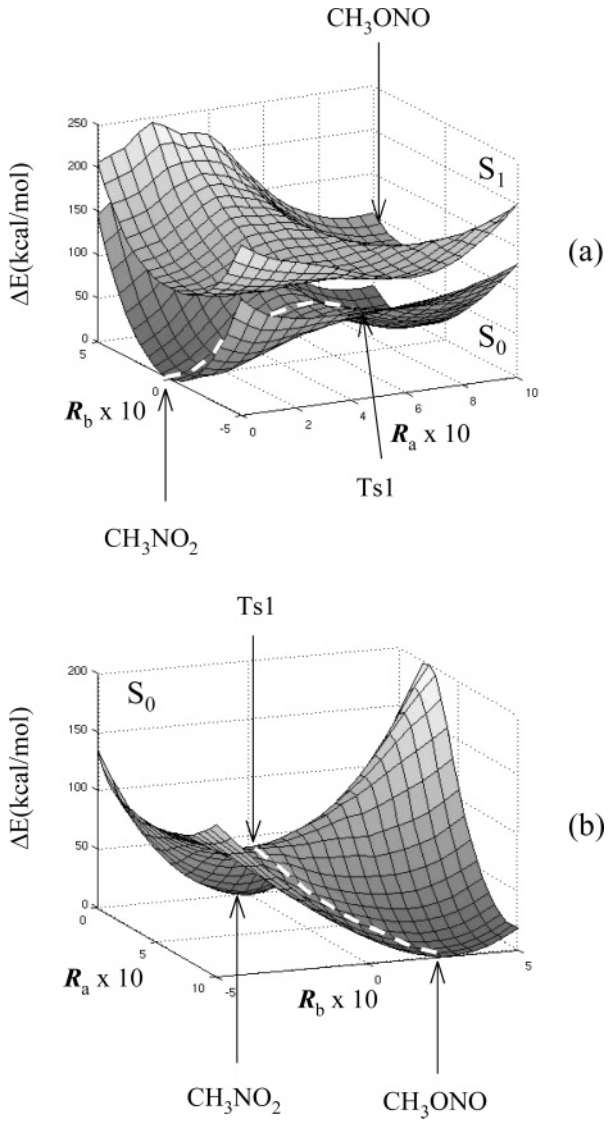


**Figure 5.** Potential energy surfaces for the $CH_2NO_2 \rightarrow CH_3ONO$ reaction (a) state average CAS-SCF/ANO-L (C,N,O[3*s*2*p*1*d*]/H[2*s*1*p*]) surfaces of the $S_1$ and $S_0$ states and (b) $S_0$ surface from a different perspective.

To finish this section, we have checked that dynamic correlation effects do not largely affect the conical intersection localized at the CAS−SCF level of theory. Thus, we have performed single point CASPT2 calculations at the most significant geometries and have found that the energy gap between the $S_0$ and $S_1$ surfaces is still small (∼1 kcal/mol) at the CASPT2 level. These calculations are illustrated in Figure S4 that shows the energy profile connecting $NH_2NO_2$ minimum with Ci1.

## Conclusions

In the present work we have investigated the potential energy surfaces related to nitro-nitrite isomerization of nitramide and nitromethane, respectively. The values predicted by the CASPT2 method for the geometrical parameters of nitromethane and methylnitrite are in excellent agreement with the experimental parameters.[32,33] More discrepancies between theoretical and experimental geometries are found in the case of nitramide.[34] Tables of the CASPT2 geometrical parameters of all the species considered in this work are given in the Supporting Information (Tables S2−S5). Additionally, we have studied the stability of the R−$NO_2$ and RO−NO bonds for both nitro and nitrite compounds. It is found that the latter one is rather weak. Therefore, whether nitrite isomer is formed in a direct reaction or not, it rapidly decomposes to RO + NO.

The main conclusion of this study is that there is no minimum energy path for rearrangement of nitramide to $NH_2ONO$. $NH_2$-ONO is formed after recombination of the $NH_2$ and $NO_2$ radicals. Furthermore, such a recombination is not barrierless. It is worthy to notice that it should be dynamically possible to find a direct isomerization path without involving a transition state, as it is suggested in recent articles.[35−37] The proposed reaction mechanism for nitramide differs from that found in nitromethane, which certainly can isomerize to methylnitrite in a one-step reaction. The reason for these different mechanistic behaviors can be understood by comparing the $S_0$ and $S_1$ potential energy surfaces of the $NH_2NO_2$−$NH_2ONO$ and $CH_3$-$NO_2$−$CH_3ONO$ systems. The presence of an $S_1/S_0$ conical intersection in the $NH_2NO_2$−$NH_2ONO$ system, which is absent in $CH_3NO_2$−$CH_3ONO$, causes a topological alteration of the potential energy surface destroying the minimum energy path for nitro-nitrite isomerization of $NH_2NO_2$.

**Acknowledgment.** This research has been supported by the Spanish Ministerio de Educación y Ciencia (Project BQU2003-1426). The authors thank SCAI (University of Málaga) for economical support to update the MOLCAS 6.2 software package. One of us, Daniel Peláez, thanks the Spanish Ministerio de Educación y Ciencia for the Grant BES-2004-6033.

**Supporting Information Available:** CASPT2 tables of energetic and geometrical parameters, intrinsic reaction coordinates, and linear interpolations. This material is available free of charge via the Internet at http://pubs.acs.org.

## References and Notes

(1) In *Conical Intersections: Electronic Structure, Dynamics and Spectroscopy*; Domcke, W., Yarkony, D. R., Köppel, H., Eds.; World Scientific: New Jersey, 2003.
(2) Worth, G. A.; Cederbaum, L. S. *Annu. Rev. Phys. Chem.* **2004**, *55*, 127.
(3) Atchity, G. J.; Xantheas, S. S.; Ruedenberg, K. *J. Chem. Phys.* **1991**, *95*, 1862.
(4) Manthe, U.; Köppel, H. *J. Chem. Phys.* **1990**, *93*, 1658.
(5) Martínez, T. J. *Chem. Phys. Lett.* **1997**, *272*, 139.
(6) Butler, L. J. *Annu. Rev. Phys. Chem.* **1998**, *49*, 125.
(7) Forde, N. R.; Myers, T. L.; Butler, L. J. *Faraday Discuss.* **1997**, *108*, 221.
(8) Waschewsky, G. C. G.; Kash, P. W.; Myers, T. L.; Kitchen, D. C.; Butler, L. J. *J. Chem. Soc., Faraday Trans.* **1994**, *90*, 1581.
(9) Blancafort, L.; Hunt, P.; Robb, M. A. *J. Am. Chem. Soc.* **2005**, *127*, 3391.
(10) Ko, C.; Levine, B.; Toniolo, A.; Manohar, L.; Olsen, S.; Werner, H.-J.; Martínez, T. J. *J. Am. Chem. Soc.* **2003**, *125*, 12710.
(11) Chaban, G.; Gordon, M. S.; Yarkony, D. R. *J. Phys. Chem. A* **1997**, *101*, 7953.
(12) Dewar, M. J. S.; Ritchie, J. P.; Alster, J. *J. Org. Chem.* **1985**, *50*, 1031.
(13) (a) Mckee, M. L. *J. Am. Chem. Soc.* **1986**, *108*, 5784. (b) Mckee, M. L. *J. Phys. Chem.* **1989**, *93*, 7365.
(14) Saxon, R. P.; Yoshimine, M. *Can. J. Chem.* **1992**, *70*, 572.
(15) Hu, W.-F.; He, T.-J.; Chen, D.-M.; Liu, F.-C. *J. Phys. Chem. A* **2002**, *106*, 7294.
(16) Nguyen M. T.; Le, H. T.; Hajgató, B.; Veszprémi, T.; Lin, M. C. *J. Phys. Chem. A* **2003**, *107*, 4286.
(17) (a) Arenas, J. F.; Otero, J. C.; Peláez, D.; Soto, J.; Serrano-Andrés, L. *J. Chem. Phys.* **2004**, *121*, 4127. (b) Arenas, J. F.; Centeno, S. P.; López-Tocón, I.; Peláez, D.; Soto, J. *J. Mol. Struct. (THEOCHEM)* **2003**, *630*, 17.
(18) Saxon, R. P.; Yoshimine, M. *J. Phys. Chem.* **1989**, *93*, 3130.
(19) Mebel, A. M.; Hsu, C.-C.; Lin, M. C.; Morokuma, K. *J. Chem. Phys.* **1995**, *103*, 5640.
(20) Velardez, G. F.; Alavi, S.; Thompson, D. L. *J. Chem. Phys.* **2005**, *123*, 074313.

(21) (a) Wodtke, A. M.; Hintsa, E. J.; Lee, Y. T. *J. Phys. Chem*. **1986**, *90*, 3549. (b) Wodtke, A. M.; Hintsa, E. J.; Lee, Y. T. *J. Chem. Phys.* **1986**, *84*, 1044.

(22) Widmark, P.-O.; Malmqvist, P.-Å.; Roos, B. O. *Theor. Chim. Acta* **1990**, *77*, 291.

(23) Roos, B. O. In *Advances in Chemical Physics; Ab Initio Methods in Quantum Chemistry II*; Lawley, K. P., Ed.; John Wiley & Sons: Chichester, England, 1987; Chapter 69, p 399.

(24) (a) Anderson, K.; Malmqvist, P.-Å.; Roos, B. O.; Sadlej, A. J.; Wolinski, K. *J. Phys. Chem.* **1990**, *94*, 5483. (b) Anderson, K.; Malmqvist, P.-Å.; Roos, B. O. *J. Chem. Phys.* **1992**, *96*, 1218.

(25) Andersson, K. et al. *MOLCAS Version 6.2*; Lund University, Sweden.

(26) Frisch, M. J.; et al. *Gaussian 03, Revision B.04*.

(27) Dunning, T. H., Jr. *J. Chem. Phys.* **1989**, *90*, 1007.

(28) Yarkony, D. R. *J. Chem. Phys.* **1990**, *92*, 2457.

(29) (a) Arenas, J. F.; Otero, J. C.; Peláez, D.; Soto, J. *J. Chem. Phys*. **2005**, *122*, 084324. (b) Arenas, J. F.; Otero, J. C.; Peláez, D.; Soto, J. *J. Phys. Chem. A* **2005**, *109*, 7172. (c) Arenas, J. F.; Otero, J. C.; Peláez, D.; Soto, J. *J. Chem. Phys.* **2003**, *119*, 7814.

(30) Bode, B. M.; Gordon, M. S. *J. Mol. Graphics Modell.* **1999**, *16*, 133.

(31) Arenas, J. F.; Otero, J. C.; Peláez, D.; Soto, J. *J. Org. Chem*. **2006**, *71*, 983.

(32) Cox, P. A.; Waring, S. *J. Chem. Soc., Faraday Trans. 2* **1972**, *68*, 1060.

(33) (a) Turner, P. H.; Corkill, M. J.; Cox, A. P. *J. Phys. Chem*. **1979**, *83*, 1473. (b) Veken, B. J.; Maas, R.; Guirgis, G. A.; Stidham, G. A.; Sheehan, T. G.; Durig, J. R. *J. Phys. Chem*. **1990**, *94*, 4026.

(34) (a) Tyler, J. K. *J. Mol. Spectrosc.* **1963**, *11*, 39. (b) Sadova, N. I.; Slepnev, G. E.; Tarasenko, N. A.; Zenkin, A. A.; Vilkov, L. V.; Shishkov, I. F.; Pankrushev, Yu. A. *Zh. Strukt. Khim.* **1977**, *18*, 865.

(35) Marcy, T. P.; Díaz, R. R.; Heard, D.; Leone, S. R.; Harding, L. B.; Klippenstein, S. J. *J. Phys. Chem. A* **2001**, *105*, 8361.

(36) Ammal, S. C.; Yamataka, H.; Aida, M.; Dupuis, M. *Science* **2003**, *299*, 1555.

(37) Towsend, D.; Lahankar, S. A.; Lee, S. K.; Chambreau, S. D.; Suits, A. G.; Zhang, X.; Rheinecker, J.; Harding, L. B.; Bowman, J. M. *Science* **2004**, *306*, 1158.